Conformationally Flexible Ellagitannins: Conformational Analysis of Davidiin and Punicafolin via DFT Calculation of ^{1}H NMR Coupling Constants

Yosuke Matsuo,[†#*] Misato Iki,[†#] Chiho Okubo,[‡#] Yoshinori Saito,[†] Takashi Tanaka[†*]

[†] Graduate School of Biomedical Sciences, Nagasaki University, 1-14 Bunkyo-machi, Nagasaki 852-8521, Japan
[‡] School of Pharmaceutical Sciences, Nagasaki University, 1-14 Bunkyo-machi, Nagasaki 852-8521, Japan

ABSTRACT: Many ellagitannins with various conformations of their glucose moiety have been isolated from natural sources. Here, a conformational analysis was performed via the density functional theory calculation of ^{1}H NMR coupling constants. It was observed that, in the solution state, davidiin exists as an equilibrium mixture of the $B_{0,3}$ (boat) and $^1C_4$ (chair) conformational states, while punicafolin is an equilibrium mixture of the $^3S_1$ (skew-boat) and $^1C_4$ conformational states. Their equilibrium states changed depending on the solvent and temperature. Such conformational flexibility may be important for the biosynthesis of ellagitannins with diverse structures.

INTRODUCTION

Hydrolyzable tannins, comprising gallotannins and ellagitannins, are a group of plant polyphenols with structural diversity and various biological activities.[1] Most ellagitannins comprise a glucose core and acyl groups, mainly hexahydroxydiphenoyl (HHDP) and dehydrohexahydroxydiphenoyl (DHHDP) groups, derived from gallic acid.[1] Feldman *et al*. suggested that the DHHDP group is oxidatively biosynthesized from galloyl groups via intramolecular coupling.[2] In addition, the DHHDP group can be converted into the HHDP group by chemical reduction.[2a,3] Our group recently reported that the DHHDP group is reductively metabolized to the HHDP group in several plants.[4] Furthermore, the DHHDP group can be produced by the $CuCl_2$-mediated oxidation of galloyl ester derivatives in aqueous media.[5] This strongly indicates that the DHHDP group is the initial product of the oxidative coupling of two galloyl groups during ellagitannin biosynthesis, and the subsequent reductive metabolism yields HHDP esters (Figure 1a).[4,5]

Glucose derivatives can adopt various conformations, such as chair (*C*), boat (*B*), skew- or twist-boat (*S*), envelope (*E*), and half-chair (*H*).[6] Many ellagitannins are presumably biosynthesized from a common precursor, 1,2,3,4,6-penta-*O*-galloyl-β-D-glucose (**1**) with a $^4C_1$ conformation (Figure 1b).[3a,7] For example, the glucose moiety of 1-β-*O*-galloylpedunculagin (casuarictin) with 2,3-(*S*)-HHDP and 4,6-(*S*)-HHDP groups exhibits the same $^4C_1$ conformation as **1**.[7] Oppositely, the glucose moiety of geraniin (**2**) with 3,6-(*R*)-HHDP and 2,4-(*R*)-DHHDP groups exhibits the $^1C_4$ conformation, where all the substituents are in the axial orientation.[4c,8] In addition, amariin (**3**) with 2,4-(*R*)-DHHDP and 3,6-(*R*)-DHHDP groups exhibits an $^{0,3}B$ conformation,[4c] whereas phyllanemblinin B (**4**) with a 2,4-(*R*)-HHDP group exhibits a $^3S_1$ conformation.[9] However, the precise conformations of several ellagitannins remain unclear. Furthermore, certain ellagitannins change their conformation depending on the solvent.[10,11]

Davidiin (**5**), an ellagitannin with 1,6-(*S*)-HHDP and 2,3,4-trigalloyl groups, has been isolated from *Davidia involucrata*,[3a,12] *Acer saccharum*,[13] and *Persicaria capitata (Polygonum capitatum)*.[14] In addition, its various biological activities have been reported.[12b,14a,15] The conformation of its glucose moiety was initially assumed to be skew-boat.[3a] However, this has not been investigated. Previous literature has depicted **5** in three conformation types, $^1C_4$,[7b–d,f,16] $^3S_1$,[17] and $B_{0,3}$,[12b,14b,18] thereby generating confusion (Figure S1). Among them, the $B_{0,3}$-type conformation was estimated from its experimental ^{1}H NMR coupling constants ($J_{H,H}$).[12b,14b,18]

Punicafolin (**6**), an ellagitannin with 3,6-(*R*)-HHDP and 1,2,4-trigalloyl groups, has been isolated from *Punica granatum*,[19] *Mallotus japonicus*,[20] *Euphorbia helioscopia*,[21] *Macaranga tanarius*,[3c] and *Phyllanthus emblica*.[9b] It exhibits several biological activities.[22] Its glucose moiety was initially assumed to exhibit a $^1C_4$ or skew-boat conformation in acetone-d_6.[19] Thereafter, it was suggested to exhibit the $B_{1,4}$ conformation in DMSO-d_6 from the $J_{H,H}$ values.[23] In several reviews, its conformation has been described as $^1C_4$.[7d,f] Recently, density functional theory (DFT) calculations have shown that its most stable conformation is $^1C_4$.[24] However, its experimental $J_{H,H}$ values in acetone-d_6 do not match those of geraniin with the $^1C_4$ conformation (Table S2).

Corilagin (**7**), an analogue of **5** without the galloyl groups at C-2 and C-4, is an ellagitannin with a flexible conformation. It reportedly exists in an intermediate state between the $B_{1,4}$ and $^{0,3}B$ (or $^1C_4$) conformations in DMSO-d_6, while a slightly perturbed $^{0,3}B$ (or $^1C_4$) conformational state in acetone-d_6.[10a,b] Its $J_{H,H}$ values change in DMSO-d_6 depending on the temperature.[10a] Compound **7** was suggested to exhibit the $^1C_4$ conformation with possible flattening of the pyranose ring at C-1 and O-5[3a] or the $B_{1,4}$ conformation[23] in

DMSO-d_6, and the $^1C_4$ conformation in acetone-d_6[8a] and CD_3OD.[8c] Furthermore, several computational studies have been conducted on the lowest-energy conformer of **7**. The molecular mechanics (PIMM91) calculation of its model compound indicated $^1C_4$.[25] The other molecular mechanics (MM2) study of **7** suggested the skew-boat conformation,[26,27] and the semiempirical PM3 calculation suggested $B_{1,4}$ as its lowest-energy conformation.[28] Based on electronic and vibrational CD spectroscopic data, $J_{H,H}$ values, and DFT calculations, a recent study reported the presence of **5** in the $^3S_1$ and $^1C_4$ conformations in DMSO-d_6 and CD_3OD, respectively.[10c,29] Notably, the conformations of 3,6-bridged glucose derivatives change depending on their substituent groups and the bridge length.[30]

To understand the biosynthetic mechanism and biological activities of ellagitannins, it is important to clarify their precise conformations. The $J_{H,H}$ values are the most useful data for the accurate determination of the conformation of glucose derivatives because they reflect the dihedral angles between vicinal hydrogens. Here, the precise conformations of **5**, **6**, and related ellagitannins in the solution state were investigated via the DFT calculations of $J_{H,H}$ values.

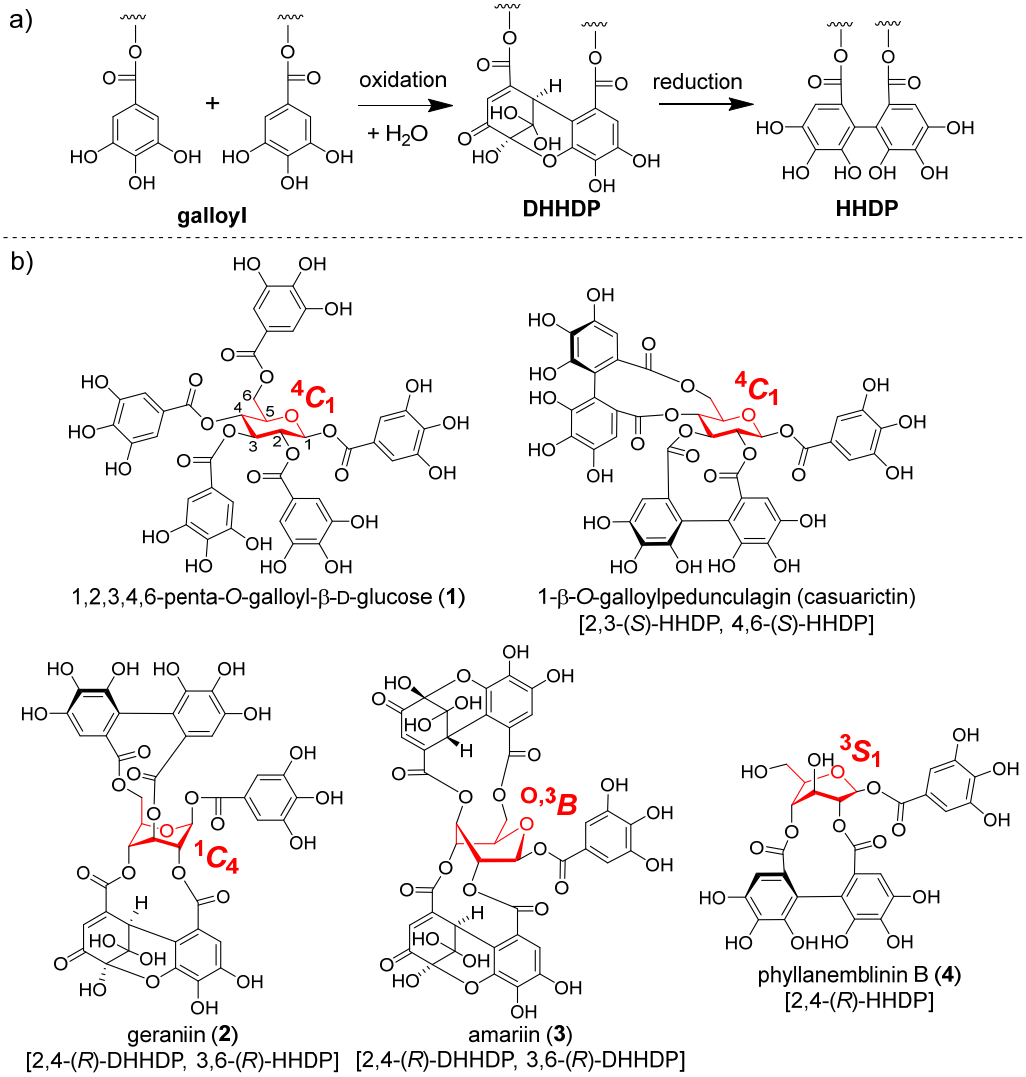

Figure 1. (a) Plausible biosynthetic pathway of dehydrohexahydroxydiphenoyl (DHHDP) and hexahydroxydiphenoyl (HHDP) groups. (b) Structures of hydrolyzable tannins with various conformations.

RESULTS AND DISCUSSION

Conformational Analysis Procedure. The conformational analysis of the ellagitannins was performed as follows. Ellagitannins possess many phenolic hydroxy groups; therefore, numerous possible conformers with different orientations of such groups exist. First, a conformational search for the molecular skeletons was performed by the ring-flipping of glucopyranose and macrocyclic structures comprising HHDP esters without considering the orientations of the hydroxy groups using the MMFF94 force field. Thereafter, the obtained conformers were optimized at the

B3LYP/6-31G(d,p) level and classified based on the conformation of glucopyranose. Second, a conformational search, including the orientation of the hydroxy groups, was performed for the lowest-energy conformers of each classified group. The conformers discovered for each group within 6 kcal/mol were optimized at the same DFT level. Their $J_{H,H}$ values with Boltzmann populations exceeding 1% were calculated at the B3LYP/6-31G(d,p)u+1s level using only the Fermi contact term.[31] Finally, the $J_{H,H}$ values were weight-averaged for each conformer group.

This procedure was first applied to phyllanemblinin B (**4**), an ellagitannin with a relatively simple structure. The conformation of its glucose moiety was originally reported to be skew-boat.[9b] Subsequently, Wakamori *et al.* suggested the $^3S_1$ type based on experimental $J_{H,H}$ values and Merck Molecular Force Field (MMFF) calculations.[9a,32] The present conformational analysis suggested three conformational states for **4**: $^3S_1$ (ΔG = 0.0 kcal/mol), $B_{1,4}$ (ΔG = +4.8 kcal/mol), and $^1C_4$ (ΔG = +5.4 kcal/mol) (B3LYP/6-31G(d,p)) (Figure S45, Table S9). Their $J_{H,H}$ values were calculated by DFT. The results for the $^3S_1$ type with the lowest-free energy were consistent with the experimental values[9a] (Table 1), indicating that the conformation of the glucose moiety was $^3S_1$.

Table 1. Experimental and calculated $J_{H,H}$ values (Hz) for phyllanemblinin B (**4**).

	exptl[a]	calcd[b]		
		$^3S_1$	$B_{1,4}$	$^1C_4$
$J_{1,2}$	5.9	6.2	7.5	0.5
$J_{2,3}$	1.0	0.7	0.9	1.3
$J_{3,4}$	3.7	3.7	3.0	3.2
$J_{4,5}$	≈ 0	0.2	0.8	1.7

[a] 500 MHz (Ref. 9a). [b] Calculated at the B3LYP/6-31G(d,p)u+1s//B3LYP/6-31G(d,p) level.

Conformational Analysis of Davidiin (5). As mentioned above, three conformers have been reported for davidiin (**5**): $^1C_4$, $^3S_1$, and $B_{0,3}$ (Figure S1). However, the experimental $J_{H,H}$ values of its glucose moiety in acetone-d_6, an NMR solvent used in previous studies,[3a,13,17a] do not match those reported for geraniin (**2**) with the $^1C_4$ conformation[8c] and **4** with the $^3S_1$ conformation[9a] (Table S1). Here, the conformational analysis of **5** revealed three types of conformations of the glucose moiety: $^1C_4$ (ΔG = 0.0 kcal/mol), $^{1,4}B$–$^1S_5$ (between $^{1,4}B$ and $^1S_5$) (ΔG = +2.8 kcal/mol), and $B_{0,3}$ (ΔG = +4.4 kcal/mol)[33] (B3LYP/6-31G(d,p)) (Figure 2, Table S13). The DFT calculation of the $J_{H,H}$ values of these conformers was performed. However, none of the results agreed with the experimental values in acetone-d_6 (Table 2), indicating that **5** does not exhibit only one conformational state. When the calculated values for $B_{0,3}$ and $^1C_4$ were weight-averaged at a ratio of 60:40, they agreed well with the experimental data (Table 2), revealing that **5** exists as an equilibrium mixture of $B_{0,3}$/$^1C_4$ in acetone-d_6. Furthermore, the weight-averaged values of the $B_{0,3}$/$^1C_4$/$^{1,4}B$–$^1S_5$ mixture (55:40:5) were in better agreement with the experimental data than those of $B_{0,3}$/$^1C_4$ (60:40) (Table 2). This suggested that the $^{1,4}B$–$^1S_5$ conformation might have slightly contributed to the equilibrium state of **5**. Moreover, the $J_{1,2}$, $J_{2,3}$, and $J_{3,4}$ values increased with a decrease in temperature (Table S3), indicating a corresponding increase in the abundance ratio of $B_{0,3}$. The ^{1}H NMR spectra of **5** were recorded in other solvents: CD_3OD, DMSO-d_6, and D_2O (Figure 3a). The experimental $J_{H,H}$ values in CD_3OD were extremely similar to those in acetone-d_6 (Table 2). Contrarily, the experimental values of $J_{1,2}$, $J_{2,3}$, $J_{3,4}$, and $J_{4,5}$ in DMSO-d_6 were higher than those in acetone-d_6 and CD_3OD. Considering that the experimental $J_{H,H}$ values in DMSO-d_6 matched the calculated values for $B_{0,3}$ (Table 2), the conformation of **5** in this solvent was identified to be $B_{0,3}$. The ^{1}H NMR spectrum in D_2O at 20°C revealed largely broadened signals, indicating a slow exchange rate between several types of conformers compared with the spectra in other solvents. Oppositely, sharp signals were observed at 80°C, and the small values of $J_{1,2}$, $J_{2,3}$, and $J_{3,4}$ indicated the $^1C_4$ conformation (Figure 3b and Table 2).

When geometry optimization including the solvent effect was performed using the polarizable continuum model (PCM),[34] the lowest-energy conformer was $^1C_4$ in all the solvents used, which was the same as without the solvent effect. The relative free energies between the three conformational groups were smaller than those without the solvent effect (Table S13). Another solvent model, the solvation model based on density (SMD),[35] which reportedly affords better results than the PCM for polar and flexible molecules, including intramolecular hydrogen bonding,[36] was applied. $B_{0,3}$ was the most stable conformation in all the solvents (Table S14). Intramolecular hydrogen bonding and intermolecular interactions with solvents seem to contribute largely to the conformation of **5**. The PCM is known to overestimate the stabilization by intramolecular hydrogen bonding.[36,37] Thus, the stabilization by intramolecular hydrogen bonds between HHDP and 3-galloyl groups in $^1C_4$ and $^{1,4}B$–$^1S_5$ and between 2- and 4-galloyl groups in $^1C_4$ appeared to be overestimated (Figure 2). These results showed that it is difficult to predict the precise conformation in various solvents based only on the calculated relative free energies, even when the solvent effect is included. However, it was possible by comparing the experimental and calculated $J_{H,H}$ values, even when the compounds existed as an equilibrium mixture of several conformations.[38]

Geometry optimization using the B3LYP-D3(BJ) functional, including long-range dispersion correction, was performed.[39-41] The results showed that the $^1C_4$ conformation (ΔG = 0.0 kcal/mol) was significantly stable compared with the $B_{0,3}$ (ΔG = +13.7 kcal/mol) and $^{1,4}B$–$^1S_5$ (ΔG = +11.7 kcal/mol) conformations (Table S13). In the $^1C_4$ conformation calculated at this level, an intramolecular π–π interaction was formed between the HHDP and 3-galloyl groups (Figure S52). Thus, in D_2O, this interaction was presumably induced by hydrophobic interactions that stabilized the $^1C_4$ conformation. However, in DMSO-d_6, the hydroxy groups in **5** formed intermolecular hydrogen bonds with the solvent, which may have hindered intramolecular interactions between the acyl groups. These results indicate that **5** has several types of conformers ($B_{0,3}$, $^1C_4$, and $^{1,4}B$–$^1S_5$), and its equilibrium state changes depending on the solvent and temperature (Table 3).

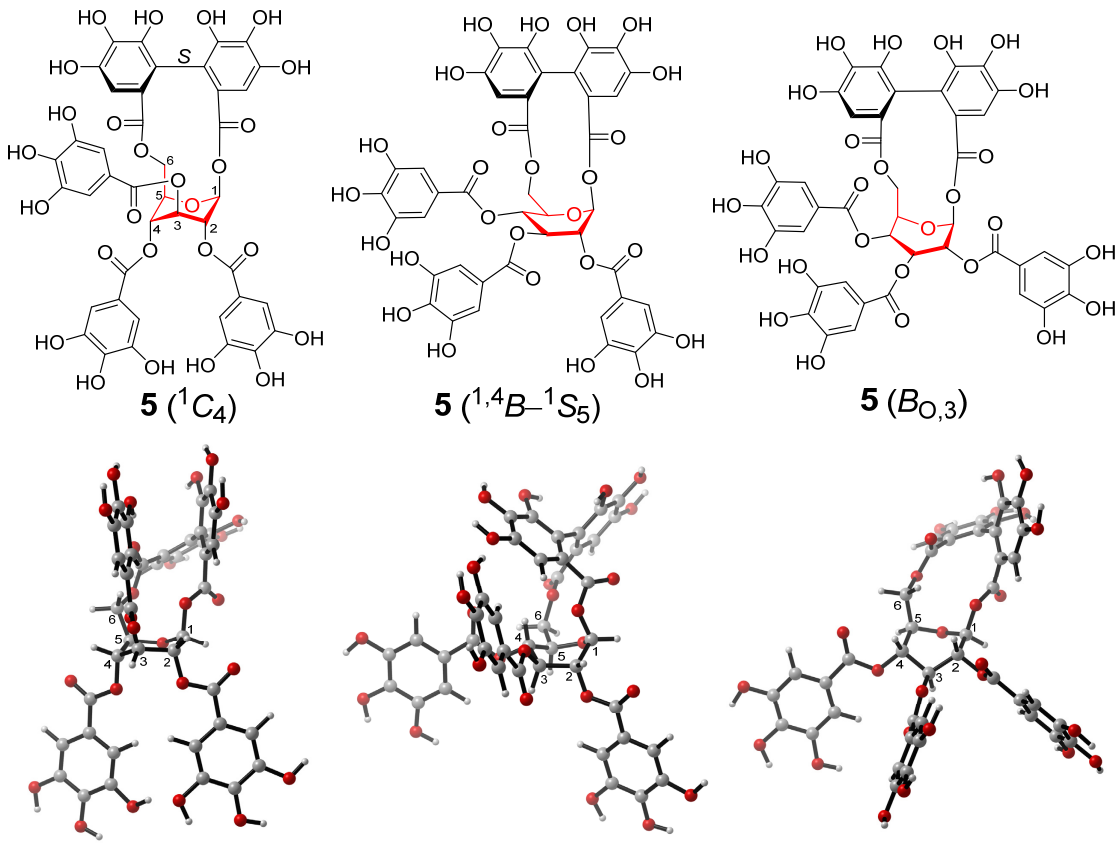

Figure 2. Three conformation types of davidiin (**5**) calculated at the B3LYP/6-31G(d,p) level.

Table 2. Experimental and calculated $J_{H,H}$ values for davidiin (**5**).

	exptl[a]				calcd[d]				
	acetone-d_6[b]	CD_3OD[b]	DMSO-d_6[b]	D_2O[c]	$^1C_4$	$^{1,4}B$–$^1S_5$	$B_{O,3}$	$B_{O,3}/^1C_4$ (60:40)	$B_{O,3}/^1C_4/^{1,4}B$–$^1S_5$ (55:40:5)
$J_{1,2}$	2.9	2.9	4.0	≈ 0	0.8	2.2	4.1	2.8	2.7
$J_{2,3}$	7.3	7.1	10.2	≈ 0	2.1	0.3	11.5	7.7	7.2
$J_{3,4}$	6.7	6.4	8.9	≈ 0	2.2	7.4	9.7	6.7	6.6
$J_{4,5}$	2.6	2.5	3.5	≈ 0	0.5	11.5	3.3	2.2	2.6
$J_{5,6a}$	5.3	5.1	4.7	5.2	5.4	4.9	4.8	5.1	5.1
$J_{5,6b}$	12.1	11.8	11.9	12.1	12.7	0.2	12.6	12.7	12.0

[a] 500 MHz, [b] 20 °C. [c] 80 °C. [d] Calculated at the B3LYP/6-31G(d,p)u+1s//B3LYP/6-31G(d,p) level.

Table 3. Conformations of davidiin (**5**), punicafolin (**6**), and corilagin (**7**) in various solvents assigned from experimental (20°C) and calculated $J_{H,H}$ values.

	acetone-d_6	CD_3OD	DMSO-d_6	D_2O
davidiin (**5**)	$B_{O,3}/^1C_4$ (60:40) [or $B_{O,3}/^1C_4/^{1,4}B$–$^1S_5$ (55:40:5)]	$B_{O,3}/^1C_4$ (60:40) [or $B_{O,3}/^1C_4/^{1,4}B$–$^1S_5$ (55:40:5)]	$B_{O,3}$	$^1C_4$[a]
punicafolin (**6**)	$^3S_1/^1C_4$ (65:35)	$^3S_1/^1C_4$ (55:45)	$^3S_1/^1C_4$ (90:10)	$^1C_4$[b]
corilagin (**7**)	$^3S_1/^1C_4$ (10:90)	$^3S_1/^1C_4$ (10:90)	$^3S_1/^1C_4$ (95:5)	$^1C_4$

[a] 80 °C. [b] D_2O/DMSO-d_6 (9:1).

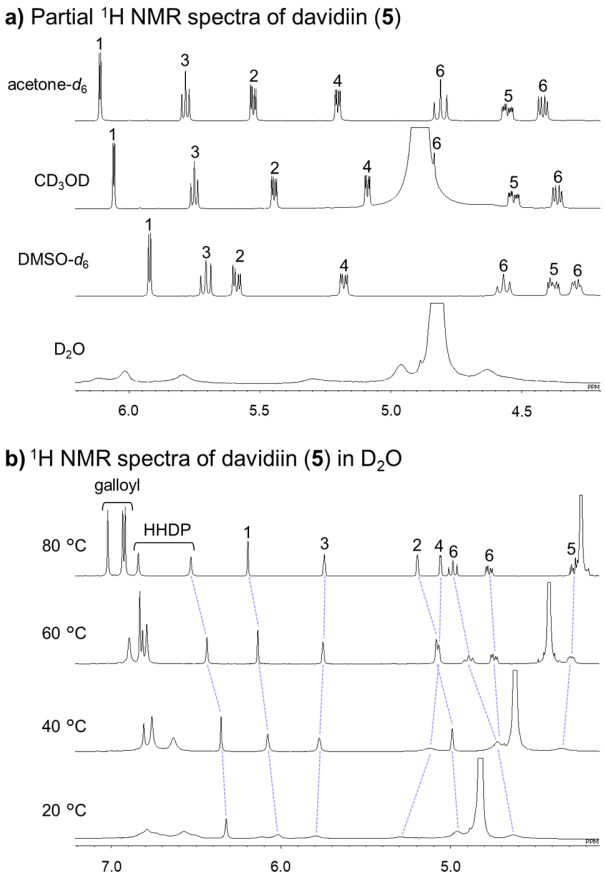

Figure 3. The ¹H NMR spectra of (a) the glucose moiety of davidiin (**5**) in various solvents at 20°C and 500 MHz and (b) **5** in D_2O at various temperatures and 500 MHz.

Conformational Analysis of Punicafolin (6) and Corilagin (7). As mentioned above, punicafolin (**6**) was originally reported to exhibit the $^1C_4$ or skew-boat conformation,[19] the former being the most stable according to recent DFT calculations.[24] Here, the conformational analysis of **6** indicated two states: $^1C_4$ (ΔG = 0.0 kcal/mol) and $^3S_1$ (ΔG = +2.6 kcal/mol) (B3LYP/6-31G(d,p)) (Figure 4, Table S22). Although the calculated $J_{H,H}$ values for both conformations did not agree with the experimental values measured in acetone-d_6, the weight-averaged values for $^3S_1/^1C_4$ (65:35) were in good agreement with the experimental values (Table 4), indicating that **6** exists as an equilibrium mixture of $^3S_1/^1C_4$ (65:35). Moreover, the $J_{1,2}$ and $J_{2,3}$ values increased with a decrease in temperature (Table S4), suggesting a corresponding increase in the abundance ratio of $^3S_1$. Furthermore, the $J_{H,H}$ values changed in different solvents, and the results revealed that **6** existed as $^3S_1/^1C_4$ (55:45) in CD_3OD, $^3S_1/^1C_4$ (90:10) in DMSO-d_6, and $^1C_4$ in D_2O/DMSO-d_6 (9:1)[42] (Figure 5a, Table 4). Geometry optimization with the solvent effect (PCM or SMD) yielded smaller relative free energies than those without the solvent effect (Tables S22, S23). However, similar to **5**, it was difficult to predict the equilibrium state of **6** in various solvents based only on the calculated relative free energies. Geometry optimization with the B3LYP-D3(BJ) functional revealed that the $^1C_4$ conformation was largely stable compared with $^3S_1$ (ΔG = 11.7 kcal/mol) (Tables S22, S23). The obtained $^1C_4$ conformer exhibited intramolecular π–π interactions between the HHDP and 1-galloyl groups and between the 2- and 4-galloyl groups (Figure S62). This indicated that such interactions were induced by hydrophobic interactions that stabilized the $^1C_4$ conformation in D_2O/DMSO-d_6 (90:10). These results indicate that **6** exhibits the $^3S_1$ and $^1C_4$ conformations, and its equilibrium state changes depending on the solvent and temperature.

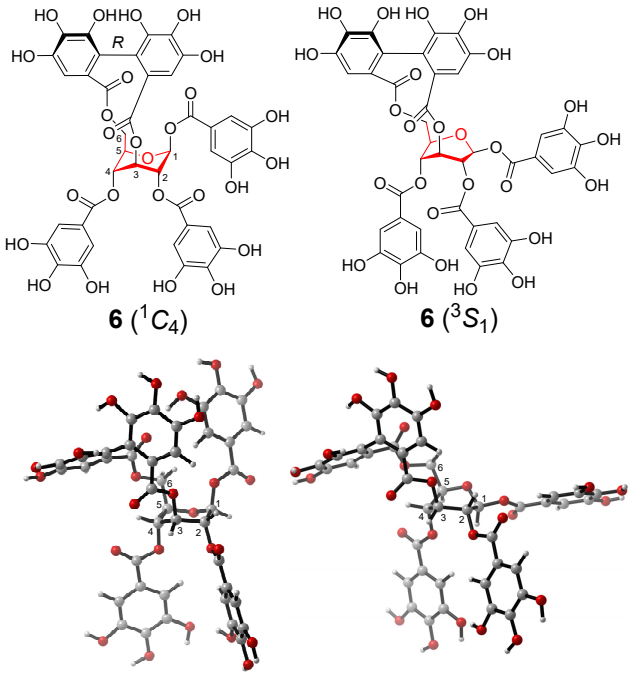

Figure 4. Two conformation types of punicafolin (**6**) calculated at the B3LYP/6-31G(d,p) level.

Table 4. Experimental and calculated $J_{H,H}$ values for punicafolin (**6**).

	exptl [a]				calcd [b]				
	acetone-d_6	CD_3OD	DMSO-d_6	D_2O/DMSO-d_6 (9:1)	$^1C_4$	$^3S_1$	$^3S_1/^1C_4$ (55:45)	$^3S_1/^1C_4$ (65:35)	$^3S_1/^1C_4$ (90:10)
$J_{1,2}$	5.1	4.5	7.1	≈ 0	0.7	7.7	4.5	5.2	7.0
$J_{2,3}$	≈ 0	≈ 0	≈ 0	≈ 0	1.8	0.4	1.0	0.9	0.6
$J_{3,4}$	3.3	3.2	3.2	3.1	2.7	3.3	3.0	3.1	3.3
$J_{4,5}$	≈ 0	≈ 0	≈ 0	≈ 0	1.0	0.3	0.6	0.5	0.4
$J_{5,6a}$	7.0	– [c]	5.6	7.5	8.1	8.1	8.1	8.1	8.1
$J_{5,6b}$	8.0	– [c]	7.8	– [c]	11.1	8.0	9.4	9.1	8.3

[a] 500 MHz, 20 °C. [b] Calculated at the B3LYP/6-31G(d,p)u+1s//B3LYP/6-31G(d,p) level. [c] Not resolved.

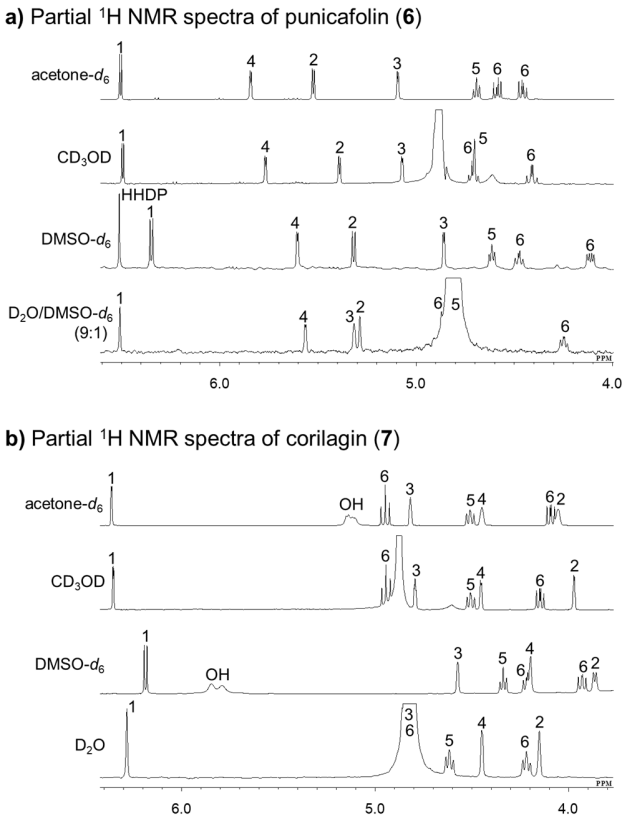

Figure 5. The ^{1}H NMR spectra of the glucose moiety of (a) punicafolin (**6**) and (b) corilagin (**7**) in various solvents at 20°C and 500 MHz.

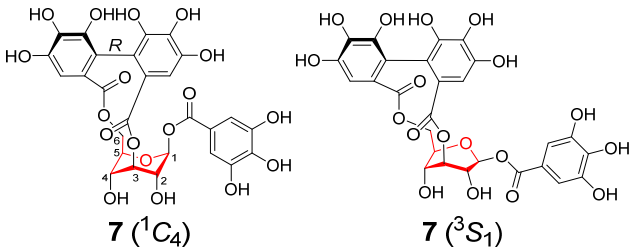

Figure 6. Two conformation types of corilagin (**7**).

The experimental $J_{H,H}$ values for corilagin (**7**) were practically the same as those for **6** in DMSO-d_6 and D_2O, suggesting that **7** also exists as an equilibrium mixture of $^3S_1$ and $^1C_4$ (Figures 5b and 6, Table S34). In acetone-d_6 and CD_3OD, its $J_{1,2}$ values (1.8 and 2.0 Hz, respectively) (Table S34) were smaller than those of **6** (5.1 and 4.5 Hz, respectively) (Table 4). This indicated a larger abundance ratio of $^1C_4$ in **7** than in **6** in the solvents. The conformational analysis afforded four types for **7**: $^1C_4$ (ΔG = 0.0 kcal/mol), $^{0,3}B$ (ΔG = +2.9 kcal/mol), $^3S_1$–$^{0,3}B$ (ΔG = +3.1 kcal/mol), and $^3S_1$ (ΔG = +4.4 kcal/mol) (Figure S65, Table S29). However, the calculated $J_{5,6}$ values for $^{0,3}B$ and $^3S_1$–$^{0,3}B$ widely differed from the experimental values (Table S34). This indicated that they do not contribute to the equilibrium state of **7**. However, the calculated $J_{H,H}$ values for $^1C_4$ and $^3S_1$ were very similar to those of **6**, except for the $J_{1,2}$ of $^3S_1$ (7.7 and 4.6 Hz for **6** and **7**, respectively) (Tables 4 and S34). In the lowest-energy $^3S_1$ conformer of **7**, an intramolecular hydrogen bond was formed between 2-hydroxy and 1-galloyl carbonyl groups, changing the dihedral angle between H-1 and H-2 (159.4° for **6** and 144.8° for **7**) (Figures 4 and S65). However, in polar solvents, hydroxy groups can form intermolecular hydrogen bonds with the solvent, and the calculated $J_{1,2}$ values for the $^3S_1$ conformations of **7**, where the 2-hydroxy groups do not form intramolecular hydrogen bonds, were practically the same as those of **6** (Figure S65, Table S34). The calculated $J_{H,H}$ values indicate that **7** exists as an equilibrium mixture of $^3S_1$ and $^1C_4$ (10:90) in acetone-d_6 and CD_3OD and as $^3S_1/^1C_4$ (95:5) in DMSO-d_6 and $^1C_4$ in D_2O (Tables 3 and S34).

The abundance ratio of the $^1C_4$ conformation of **7** was higher than that of **6** (Table 3). For **6**, the distance between O-2 and O-4 atoms in the glucose moiety was closer in $^1C_4$ (2.9 Å) than in $^3S_1$ (3.2 Å), suggesting a larger steric hindrance between the 2- and 4-galloyl groups in the $^1C_4$ conformation than in $^3S_1$. Thus, the abundance ratio of $^3S_1$ was probably higher in **6** than in **7**.

Conformational Analysis of Macaranganin (8). Macaranganin (**8**) is a diastereomer of **6** with a 3,6-(*S*)-HHDP group. It has been isolated from *Macaranga tanarius*.[3c] Its lowest-energy conformer has been identified as $^5S_1$ through DFT calculations.[24] Here, its conformational analysis indicated four possible conformational states: $^3S_1$ (ΔG = 0.0 kcal/mol), $^5S_1$–$B_{1,4}$ (ΔG = +0.6 kcal/mol), $^5S_1$–^5E (ΔG = +2.5

https://doi.org/10.26434/chemrxiv-2022-wrlxz-v3 **ORCID:** https://orcid.org/0000-0002-6462-9727

kcal/mol), and $^5S_1$ (ΔG = +4.5 kcal/mol) (B3LYP/6-31G(d,p)) (Figure S69, Table S41). The DFT calculations including the solvent effect afforded smaller relative free energies: $^3S_1$ (ΔG = 0.00 kcal/mol), $^5S_1$–$B_{1,4}$ (ΔG = +0.19 kcal/mol), $^5S_1$–^5E (ΔG = +0.90 kcal/mol), and $^5S_1$ (ΔG = +0.73 kcal/mol) (B3LYP/6-31G(d,p) in acetone (PCM)) (Table S41). The reported experimental $J_{H,H}$ values in acetone-d_6 + D_2O[24] were in good agreement with the calculated values for $^5S_1$ (Table S46). Thus, the conformation of **8** was confirmed to be $^5S_1$ (Figure 7). When the B3LYP-D3(BJ) functional was used for geometry optimization, the four types of conformers converged into two types, $^5S_1$ and $^3S_1$ (Figure S71). Considering that **8** was unavailable for the present study, it was impossible to investigate its conformations in other solvents.

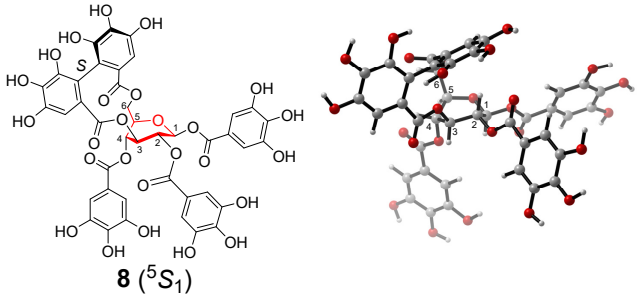

8 ($^5S_1$)

Figure 7. The $^5S_1$ conformation of macaranganin (**8**) calculated at the B3LYP/6-31G(d,p) level.

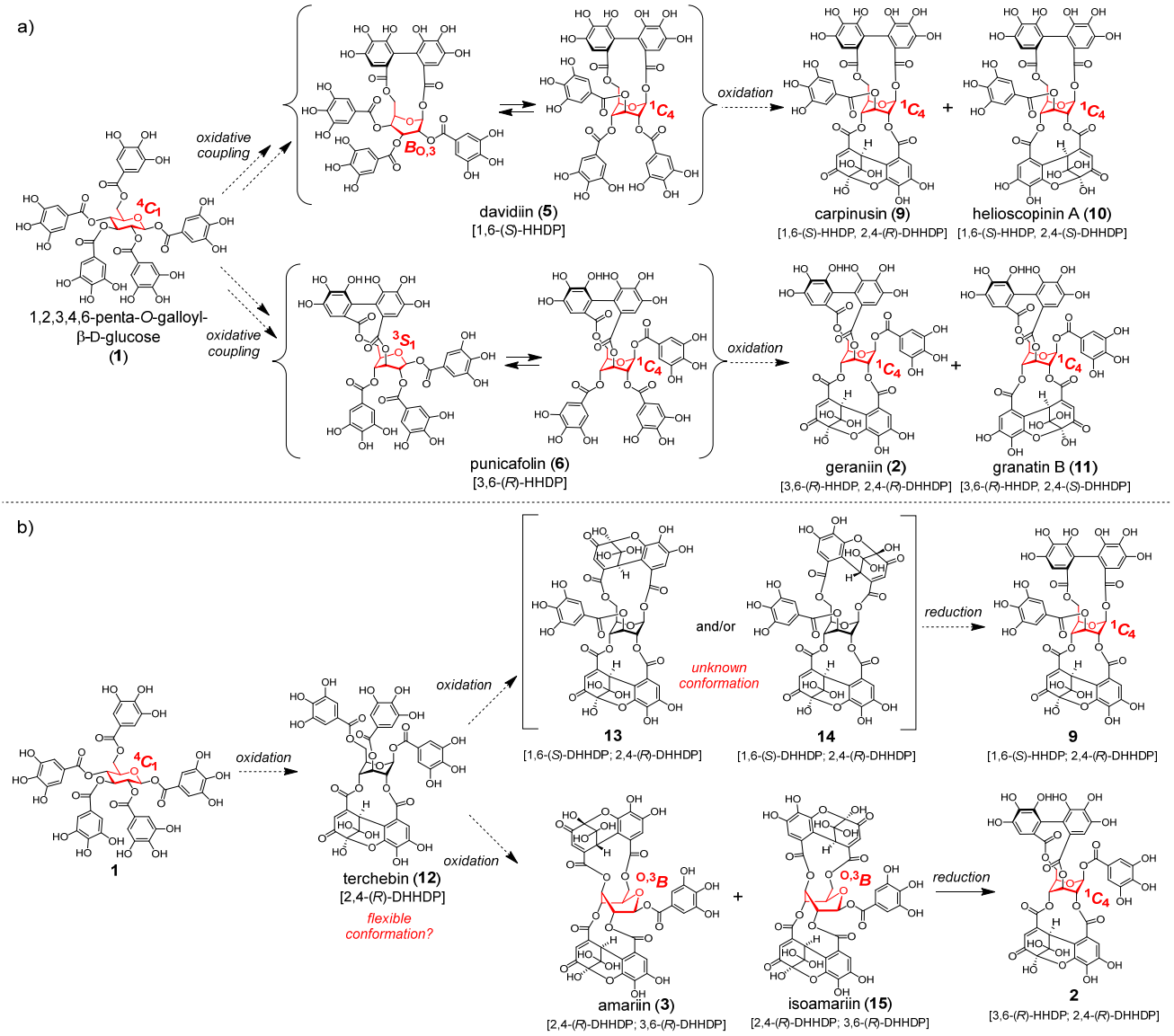

Scheme 1. Possible biosynthetic pathways toward ellagitannins **2** and **9**–**11** with the $^1C_4$ conformation from 1,2,3,4,6-penta-*O*-galloyl-β-D-glucose (**1**) (a) via the flexible-conformation intermediates **5** and **6**, and (b) via terchebin (**12**). HHDP, hexahydroxydiphenoyl; DHHDP, dehydrohexahydroxydiphenoyl.

Biosynthetic Considerations of $^1C_4$-type Ellagitannins. The conformational flexibility of ellagitannins revealed in the present study is crucial in the biosynthesis of $^1C_4$-type ellagitannins from **1** with the $^4C_1$ conformation (Scheme 1a). The conformation of carpinusin (**9**)[43] and helioscopinin A (**10**)[14b,21] with a 1,6-(*S*)-HHDP group is locked as the $^1C_4$ type by a 2,4-bridged DHHDP group. For their biosynthesis from **1**, a glucose moiety with the $^4C_1$ conformation must be converted into the $^1C_4$ type. Conformationally flexible **5** can be biosynthesized from **1** via oxidative coupling between its 1- and 6-galloyl groups. In turn, since **5** can adopt the $^1C_4$ conformation, **9** and **10** can be biosynthesized via oxidative coupling between the 2- and 4-galloyl groups in **5**. Similarly, geraniin (**2**) and granatin B (**11**),[3a,19,44] locked as the $^1C_4$ conformation by a 2,4-bridged DHHDP group, can be biosynthesized from **1** via the flexible intermediate **6**, which can adopt the $^1C_4$ conformation.

Conversely, another possible biosynthetic pathway toward $^1C_4$-type ellagitannins exists (Scheme 1b). Geraniin (**2**) is reductively biosynthesized from amariin (**3**) and isoamariin (**15**) bearing 2,4-(*R*)- and 3,6-(*R*)-DHHDP groups with the $^{0,3}B$-type conformation.[4c,45] In addition, **3** and **15** can be oxidatively biosynthesized from **1** via terchebin (**12**) bearing a 2,4-(*R*)-DHHDP group.[44a] Although the conformation of **12** has not been investigated, it was suggested to exist in an intermediate state between the $B_{1,4}$ and $^{0,3}B$ (or $^1C_4$) conformations in DMSO-d_6.[10a] We assume that **12** might also have a flexible conformation; this is currently under investigation. Compound **9** can also be biosynthesized from **12.** The formation of a DHHDP group between the 1,6-galloyl groups in **12** would afford unknown intermediates **13** and **14**, which could be reductively metabolized to produce **9**.

CONCLUSION

The precise conformations of davidiin (**5**) (bearing a 1,6-(*S*)-HHDP group) and punicafolin (**6**) (bearing a 3,6-(*R*)-HHDP group) were revealed by conformational analysis through DFT calculations of the $J_{H,H}$ values. These ellagitannins exhibited flexible conformations in the solution state, and their equilibrium states were significantly influenced by the solvent and temperature. The conformation of corilagin (**7**), which is known to change depending on the solvent, was also investigated. Here, it was difficult to predict the precise conformations of these flexible ellagitannins only from the calculated relative free energies under several calculation conditions. Although several studies have investigated the conformations of **5** and **6** using computational methods, most of them could not precisely predict them since they were based on the calculated relative (free) energies and did not consider the simultaneous existence of several conformations as an equilibrium state. However, this study demonstrated that the precise conformation can be predicted by comparing the experimental $J_{H,H}$ values with the corresponding calculated values. Recently, Auer *et al*. investigated the conformations of xylopyranoside derivatives. They demonstrated that identifying the most stable conformers using the computational calculations of relative free energies or NMR chemical shifts was not sensitive, whereas the calculation of $J_{H,H}$ values enabled the quantification of the ratio of different conformers in the mixture.[46] The procedure of conformational analysis presented here was similar to that of Auer et al.

Conformationally flexible ellagitannins are important intermediates in the biosynthesis of ellagitannins with the $^1C_4$ conformation. Their flexibility may contribute to their various biological activities. Although several in silico molecular docking studies of **5**–**7** with proteins have been reported,[47] their flexibility, as revealed here, contributes to the future bioinformatics research of these ellagitannins. Ellagitannins have attracted significant attention as targets for total syntheses because of their structural diversity and complexity.[48] For example, the total syntheses of **5**–**8** have been reported.[17a,24,49] The elucidation of the precise conformations of ellagitannins will be important for their efficient synthesis.

AUTHOR INFORMATION

Corresponding Author

* Yosuke Matsuo, E-Mail: y-matsuo@nagasaki-u.ac.jp
* Takashi Tanaka, E-Mail: t-tanaka@nagasaki-u.ac.jp

Author Contributions

# Y.M., M.I., and C.O. contributed equally to this work.

ORCID

Yosuke Matsuo: 0000-0002-6462-9727
Yoshinori Saito: 0000-0002-3587-9743
Takashi Tanaka: 0000-0001-7762-7432

Notes

The authors declare no competing financial interest.

ACKNOWLEDGMENT

This work was partly supported by JSPS KAKENHI Grant Number JP20K07102. This work was the result of using research equipment shared in the MEXT Project for promoting public utilization of advanced research infrastructure (Program for supporting introduction of the new sharing system) Grant Number JPMXS0422500320. The computation was partly carried out using the computer resource offered under the category of General Projects by the Research Institute for Information Technology, Kyushu University. The authors would like to thank Enago (www.enago.jp) for the English language review.

REFERENCES

(1) (a) Okuda, T.; Yoshida, T.; Hatano, T. Hydrolyzable Tannins and Related Polyphenols. In *Fortschritte der Chemie Organischer Naturstoffe / Progress in the Chemistry of Organic Natural Products*; Herz, W.; Kirby, G. W.; Moore, R. E.; Steglich, W.; Tamm, C., Eds.; Fortchemie, Vol. 66; Springer, 1995; pp. 1-117. DOI: 10.1007/978-3-7091-9363-1_1; (b) *Chemistry and Biology of Ellagitannins: An Underestimated Class of Bioactive Plant Polyphenols*; Quideau, S., Ed.; World Scientific Publishing, 2009. DOI: 10.1142/6795; (c) Okuda, T.; Ito, H. Tannins of constant structure in medicinal and food plants—Hydrolyzable tannins and polyphenols related to tannins. *Molecules* **2011**, *16*, 2191-2217; (d) Yamada, H.; Wakamori, S.; Hirokane, T.; Ikeuchi, K.; Matsumoto, S. Structural revisions in natural ellagitannins. *Molecules* **2018**, *23*, 1901.

(2) (a) Quideau, S.; Feldman, K. S. Ellagitannin chemistry. The first synthesis of dehydrohexahydroxydiphenoate esters from oxidative coupling of unetherified methyl gallate. *J. Org. Chem*. **1997**, *62*, 8809-8813; (b) Feldman, K. S. Recent progress in ellagitannin chemistry. *Phytochemistry* **2005**, *66*, 1984-2000.

(3) (a) Haddock, E. A.; Gupta, R. K.; Haslam, E. The metabolism of gallic acid and hexahydroxydiphenic acid in plants. Part 3. Esters of (*R*)- and (*S*)-hexahydroxydiphenic acid and dehydrohexahydroxydiphenic acid with D-glucopyranose ($^1C_4$ and related conformations). *J. Chem. Soc., Perkin Trans. 1* **1982**, 2535-2545. (b) Nonaka, G.; Matsumoto, Y.; Nishioka, I.; Nishizawa, M.; Yamagishi, T. Trapain, a new hydrolyzable tannin from *Trapa Japonica* FLEROV. *Chem. Pharm. Bull*. **1981**, *29*, 1184-1187. (c) Lin, J.-H.; Nonaka, G.; Nishioka, I. Tannins and related compounds. XCIV. Isolation and characterization of seven new hydrolyzable tannins from the leaves of *Macaranga tanarius* (L.) MUELL. *et* ARG. *Chem. Pharm. Bull*. **1990**, *38*, 1218-1223.

(4) (a) Tanaka, T. Reactions of ellagitannins related to their metabolism in higher plants. In *Recent Advances in Polyphenol Research*; Salminen, J.-P., Wähälä, K., Freitas, V., Quideau, S., Eds.; Vol. 8; Wiley-Blackwell, 2023; pp. 347-368. DOI: 10.1002/9781119844792.ch12. (b) Kojima, D.; Shimizu, K.; Aritake, K.; Era, M.; Matsuo, Y.; Saito, Y.; Tanaka, T.; Nonaka, G. Highly oxidized ellagitannins of *Carpinus japonica* and their oxidation–reduction disproportionation. *J. Nat. Prod*. **2020**, *83*, 3424-3434. (c) Era, M.; Matsuo, Y.; Saito, Y.; Tanaka, T. Production of ellagitannin hexahydroxydiphenoyl ester by spontaneous reduction of dehydrohexa-hydroxydiphenoyl ester. *Molecules* **2020**, *25*, 1051. (d) Wakamatsu, H.; Tanaka, S.; Matsuo, Y.; Saito, Y.; Nishida, K.; Tanaka, T. Reductive metabolism of ellagitannins in the young leaves of *Castanopsis sieboldii*. *Molecules* **2019**, *24*, 4279.

(5) Yamashita, T.; Matsuo, Y.; Saito, Y.; Tanaka, T. Formation of dehydrohexahydroxydiphenoyl esters by oxidative coupling of galloyl esters in an aqueous medium involved in ellagitannin biosynthesis. *Chem.—Asian J*. **2021**, *16*, 1735-1740.

(6) (a) Mayes, H. B.; Broadbelt, L. J.; Beckham, G. T. How sugars pucker: Electronic structure calculations map the kinetic landscape of five biologically paramount monosaccharides and their implications for enzymatic catalysis. *J. Am. Chem. Soc*. **2014**, *136*, 1008-1022. (b) Biarnés, X.; Ardèvol, A.; Planas, A.; Rovira, C.; Laio, A.; Parrinello, M. The conformational free energy landscape of α-D-glucopyranose. Implications for substrate preactivation in α-glucoside hydrolases. *J. Am. Chem. Soc*. **2007**, *129*, 10686-10693. (c) IUPAC-IUB Joint Commission on Biochemical Nomenclature (JCBN). Conformational nomenclature for five- and six-membered ring forms of monosaccharides and their derivatives. *Pure Appl. Chem*. **1981**, *53*, 1901-1905.

(7) (a) Gupta, R. K.; Al-Shafi, S. M. K.; Layden, K.; Haslam, E. The metabolism of gallic acid and hexahydroxydiphenic acid in plants. Part 2. Esters of (*S*)-hexahydroxydiphenic acid with D-glucopyranose ($^4C_1$). *J. Chem. Soc., Perkin Trans. 1* **1982**, 2525-2534. (b) Haslam, E. Secondary metabolism – fact and fiction. *Nat. Prod. Rep*. **1986**, *3*, 217-249. (c) Spencer, C. M.; Cai, Y.; Martin, R.; Gaffney, S. H.; Goulding, P. N.; Magnolato, D.; Lilley, T. H.; Haslam, E. Polyphenol complexation—some thoughts and observations. *Phytochemistry* **1988**, *27*, 2397-2409. (d) Haslam, E.; Cai, Y. Plant polyphenols (vegetable tannins): gallic acid metabolism. *Nat. Prod. Rep*. **1994**, *11*, 41-66. (e) Haslam, E. Taste, bitterness and astringency. in *Practical Polyphenolics: From structure to molecular recognition and physiological action*. Cambridge University Press, 1998; pp. 178-225. (f) Helm, R. F.; Zhentian, L.; Ranatunga, T.; Jervis, J.; Elder, T. Toward understanding monomeric ellagitannin biosynthesis. In *Plant Polyphenols 2: Chemistry, Biology, Pharmacology, Ecology*, Gross, G. G.; Hemingway, R. W.; Yoshida, T.; Branham, S. J., Eds.; Basic Life Sciences, Vol 66; Springer, 1999; pp. 83-99. DOI: 10.1007/978-1-4615-4139-4_5; (g) Grundhöfer, P.; Niemetz, R.; Schilling, G.; Gross, G. G. Biosynthesis and subcellular distribution of hydrolyzable tannins. *Phytochemistry* **2001**, 57, 915–927.

(8) (a) Hatano, T.; Yoshida, T.; Shingu, T.; Okuda, T. ^{13}C Nuclear magnetic resonance spectra of hydrolyzable tannins. III. Tannins having $^1C_4$ glucose and C-glucosidic linkage. *Chem. Pharm. Bull*. **1988**, *36*, 3849-3856. (b) Luger, P.; Weber, M.; Kashino, S.; Amakura, Y.; Yoshida, T.; Okuda, T.; Beurskens, G.; Dauter, Z. Structure of the tannin geraniin based on conventional X-ray data at 295 K and on synchrotron data at 293 and 120 K. *Acta Crystallogr., Sect. B: Struct. Sci*. **1998**, *B54*, 687-694. (c) Sudjaroen, Y.; Hull, W. E.; Erben, G.; Würtele, G.; Changbumrung, S.; Ulrich, C. M.; Owen, R. W. Isolation and characterization of ellagitannins as the major polyphenolic components of Longan (*Dimocarpus longan* Lour) seeds. *Phytochemistry* **2012**, *77*, 226-237.

(9) (a) Matsumoto, S.; Wakamori, S.; Nishii, K.; Tanaka, T.; Yamada, H. Total synthesis of phyllanemblinin B. *Synlett* **2020**, *31*, 1389-1393. (b) Zhang, Y.-J.; Abe, T.; Tanaka, T.; Yang, C.-R.; Kouno, I. Phyllanemblinins A–F, new ellagitannins from *Phyllanthus emblica*. *J. Nat. Prod*. **2001**, *64*, 1527-1532.

(10) (a) Jochims, J. C.; Taigel, G.; Schmidt, O. T. Über natürliche gerbstoffe, XLI. Protonenresonanz-spektren und konformationsbestimmung einiger natürlicher gerbstoffe. *Justus Liebigs Ann. Chem*. **1968**, *717*, 169-185. (b) Seikel, M. K.; Hillis, W. E. Hydrolysable tannins of *Eucalyptus delegatensis* wood. *Phytochemistry* **1970**, *9*, 1115-1128. (c) Sprenger, R. F.; Thomasi, S. S.; Ferreira, A. G.; Cass, Q. B.; Batista Junior, J. M. Solution-state conformations of natural products from chiroptical spectroscopy: the case of isocorilagin. *Org. Biomol. Chem*. **2016**, *14*, 3369-3375.

(11) Klika, K. D.; Saleem, A.; Sinkkonen, J.; Kähkönen, M.; Loponen, J.; Tähtinen, P.; Pihlaja, K. The structural and conformational analyses and antioxidant activities of chebulinic acid and its thrice-hydrolyzed derivative, 2,4-chebuloyl-β-D-glucopyranoside, isolated from the fruit of *Terminalia chebula*. *ARKIVOC* **2004**, 83-105.

(12) (a) Spencer, C. M.; Cai, Y.; Martin, R.; Lilley, T. H.; Haslam, E. The metabolism of gallic acid and hexahydroxydiophenic acid in higher plants part 4; Polyphenol interactions part 3. Spectroscopic and physical properties of esters of gallic acid and (*S*)-hexahydroxydiphenic acid with D-glucopyranose ($^4C_1$). *J. Chem. Soc., Perkin Trans. 2* **1990**, 651-660. (b) Shimozu, Y.; Kimura, Y.; Esumi, A.; Aoyama, H.; Kuroda, T.; Sakagami, H.; Hatano, T. Ellagitannins of *Davidia involucrata*. I. Structure of davicratinic acid A and effects of Davidia tannins on drug-resistant bacteria and human oral squamous cell carcinomas. *Molecules* **2017**, *22*, 470.

(13) Hatano, T.; Hattori, S.; Ikeda, Y.; Shingu, T.; Okuda, T. Gallotannins having a 1,5-anhydro-D-glucitol core and some ellagitannins from *Acer* species. *Chem. Pharm. Bull*. **1990**, *38*, 1902-1905.

(14) (a) Fu, J.; Ma, J.-Y.; Zhang, X.-F.; Wang, Y.; Feng, R.; Chen, Y.-C.; Tan, X.-S.; Zhang, Y.-Y.; Sun, Y.-P.; Zhou, Y.; Ma, C.; He, C.-Y.; Zhao, Z.-X.; Du, X.-W. Identification of metabolites of FR429, a potential antitumor ellagitannin, transformed by rat intestinal bacteria in vitro, based on liquid chromatography–ion trap-time of flight mass spectrometry analysis. *J. Pharm. Biomed. Anal*. **2012**, *71*, 162-167. (b) Li, Y.-Q.; Kitaoka, M.; Takayoshi, J.; Wang, Y.-F.; Matsuo, Y.; Saito, Y.; Huang, Y.-L.; Li, D.-P.; Nonaka, G.; Jiang, Z.-H.; Tanaka. T. Ellagitannins and oligomeric proanthocyanidins of three Polygonaceous plants. *Molecules* **2021**, *26*, 337.

(15) (a) Zhu, M.; Phillipson, J. D.; Greengrass, P. M.; Bowery, N. E.; Cai, Y. Plant polyphenols: Biologically active compounds or non-selective binders to protein? *Phytochemistry* **1997**, *44*, 441-447. (b) Wang, Y.; Ma, J.; Chow, S. C.; Li, C. H.; Xiao, Z.; Feng, R.; Fu, J.; Chen, Y. A potential antitumor ellagitannin, davidiin, inhibited hepatocellular tumor growth by targeting EZH2. *Tumor Biol*. **2014**, *35*, 205-212. (c) Takemoto, M.; Kawamura, Y.; Hirohama, M.; Yamaguchi, Y.; Handa, H.; Saitoh, H.; Nakao, Y.; Kawada, M.; Khalid, K.; Koshino, H.; Kimura, K.; Ito, A.; Yoshida, M. Inhibition of protein SUMOylation by davidiin, an ellagitannin from *Davidia involucrata*. *J. Antibiot*. **2014**, *67*, 335-338.

(16) (a) Quideau, S.; Feldman, K. S. Ellagitannin chemistry. *Chem. Rev*. **1996**, *96*, 475-503. (b) Su, X.; Thomas, G. L.; Galloway, W. R. J. D.; Surry, D. S.; Spandl, R. J.; Spring, D. R. Synthesis of biaryl-containing medium-ring systems by organocuprate oxidation: Applications in the total synthesis of ellagitannin natural products. *Synthesis* **2009**, 3880-3896.

(17) (a) Kasai, Y.; Michihata, N.; Nishimura, H.; Hirokane, T.; Yamada, H. Total synthesis of (+)-davidiin. *Angew. Chem., Int. Ed*. **2012**, *51*, 8026-8029. (b) Ashibe, S.; Ikeuchi, K.; Kume, Y.; Wakamori, S.; Ueno, Y.; Iwashita, T.; Yamada, H. Non-enzymatic oxidation of a pentagalloylglucose

analogue into members of the ellagitannin family. *Angew. Chem., Int. Ed.* **2017**, *56*, 15402-15406.

(18) In Ref. 12b, the conformation of **5** was described as skew-boat type.

(19) Tanaka, T.; Nonaka, G.; Nishioka, I. Punicafolin, an ellagitannin from the leaves of *Punica granatum*. *Phytochemistry* **1985**, *24*, 2075-2078.

(20) Saijo, R.; Nonaka, G.; Nishioka, I. Tannins and related compounds. LXXXIV. Isolation and characterization of five new hydrolyzable tannins from the bark of *Mallotus japonicus*. *Chem. Pharm. Bull*. **1989**, *37*, 2063-2070.

(21) Lee, S.-H.; Tanaka, T.; Nonaka, G.; Nishioka, I. Tannins and related compounds. XCV. Isolation and characterization of helioscopinins and helioscopins, four new hydrolyzable tannins from *Euphorbia helioscopia* L. (1). *Chem. Pharm. Bull*. **1990**, *38*, 1518-1523.

(22) (a) Kashiwada, Y.; Nonaka, G.; Nishioka, I.; Lee, K. J.-H.; Bori, I.; Fukushima, Y.; Bastow, K. F.; Lee, K.-H. Tannins as potent inhibitors of DNA topoisomerase II in vitro. *J. Pharm. Sci*. **1993**, *82*, 487-492. (b) Tanimura, S.; Kadomoto, R.; Tanaka, T.; Zhang, Y.-J.; Kouno, I.; Kohno, M. Suppression of tumor cell invasiveness by hydrolyzable tannins (plant polyphenols) via the inhibition of matrix metalloproteinase-2/-9 activity. *Biochem. Biophys. Res. Commun*. **2005**, *330*, 1306-1313. (c) Xu, M.; Zhu, H.-T.; Cheng, R.-R.; Wang, D.; Yang, C.-R.; Tanaka, T.; Kouno, I.; Zhang, Y.-J. Antioxidant and hyaluronidase inhibitory activities of diverse phenolics in *Phyllanthus emblica*. *Nat. Prod. Res*. **2016**, *30*, 2726-2729. (d) Lee, J.; Lee, S.-H.; Min, K. R.; Lee, K.-S.; Ro, J.-S.; Ryu, J.-C.; Kim, Y. Inhibitory effects of hydrolyzable tannins on Ca^{2+}-activated hyaluronidase. *Planta Med*. **1993**, *59*, 381-382. (e) Kashiwada, Y.; Huang, L.; Ballas, L. M.; Jiang, J. B.; Janzen, W. P.; Lee, K.-H. New hexahydroxybiphenyl derivatives as inhibitors of protein kinase C. *J. Med. Chem*. **1994**, *37*, 195-200.

(23) Nawwar, M. A. M.; Hussein, S. A. M.; Merfort, I. NMR spectral analysis of polyphenols from *Punica granatum*. *Phytochemistry* **1994**, *36*, 793-798.

(24) Shibayama, H.; Ueda, Y.; Tanaka, T.; Kawabata, T. Seven-step stereodivergent total syntheses of punicafolin and macaranganin. *J. Am. Chem. Soc*. **2021**, *143*, 1428-1434.

(25) Immel, S.; Khanbabaee, K. Atropdiastereoisomers of ellagitannin model compounds: configuration, conformation, and relative stability of D-glucose diphenoyl derivatives. *Tetrahedron: Asymmetry* **2000**, *11*, 2495-2507.

(26) Li,X.; Liu, J.; Chen, B.; Chen, Y.; Dai, W.; Li, Y.; Zhu, M. Covalent bridging of corilagin improves antiferroptosis activity: Comparison with 1,3,6-tri-*O*-galloyl-β-D-glucopyranose. *ACS Med. Chem. Lett.* **2020**, *11*, 2232-2237.

(27) Although **7** has a 3,6-(*R*)-HHDP group, its 3D model depicted in Ref. 26 has a 3,6-(*S*)-HHDP group.

(28) Gaudreault, R.; van de Ven, T. G. M.; Whitehead, M. A. Molecular modeling of poly(ethylene oxide) model cofactors; 1,3,6-tri-O-galloyl-β-D-glucose and corilagin. *J. Mol. Model.* **2002**, *8*, 73–80.

(29) In Ref. 10c, **7** was reported to exist as an equilibrium mixture of $B_{1,4}$ and $^3S_1$ ($^3S_1$ was incorrectly described in the literature as $^0S_5$) in DMSO-d_6; however, both two conformers depicted are considered to be close to the $^3S_1$ conformation.

(30) (a) Ikuta, D.; Hirata, Y.; Wakamori, S.; Shimada, H.; Tomabechi, Y.; Kawasaki, Y.; Ikeuchi, K.; Hagimori, T.; Matsumoto, S.; Yamada, H. Conformationally supple glucose monomers enable synthesis of the smallest cyclodextrins. *Science* **2019**, *364*, 674-677. (b) Heuckendorff, M.; Pedersen, C. M.; Bols, M. Conformationally armed 3,6-tethered glycosyl donors: Synthesis, conformation, reactivity, and selectivity. *J. Org. Chem*. **2013**, *78*, 7234-7248.

(31) Bally, T.; Rablen, P. R. Quantum-chemical simulation of ^{1}H NMR Spectra. 2. Comparison of DFT-based procedures for computing proton–proton coupling constants in organic molecules. *J. Org. Chem*. **2011**, *76*, 4818-4830.

(32) Although **4** has a 2,4-(*R*)-HHDP group, its lowest-energy conformer shown in the Supporting Information of Ref. 9a has a 2,4-(*S*)-HHDP group.

(33) Although the $B_{0,3}$ type conformer of **5** is exactly between $B_{0,3}$ and $^2S_0$, it is described as $B_{0,3}$ in this paper since it is relatively close to $B_{0,3}$.

(34) Tomasi, J.; Mennucci, B.; Cammi, R. Quantum mechanical continuum solvation models. *Chem. Rev*. **2005**, *105*, 2999-3093.

(35) Marenich, A. V.; Cramer, C. J.; Truhlar, D. G. Universal solvation model based on solute electron density and on a continuum model of the solvent defined by the bulk dielectric constant and atomic surface tensions. *J. Phys Chem. B* **2009**, *113*, 6378-6396.

(36) (a) Zanardi, M. M.; Marcarino, M. O.; Sarotti, A. M. Redefining the impact of Boltzmann analysis in the stereochemical assignment of polar and flexible molecules by NMR calculations. *Org. Lett.* **2020**, *22*, 52-56. (b) Del Vigo, E. A.; Marino, C.; Stortz, C. A. Exhaustive rotamer search of the $^4C_1$ conformation of α- and β-D-galactopyranose. *Carbohydr. Res*. **2017**, *448*, 136-147.

(37) Zanardi, M. M.; Sortino, M. A.; Sarotti, A. M. On the effect of intramolecular H-bonding in the configurational assessment of polyhydroxylated compounds with computational methods. The hyacinthacines case. *Carbohydr. Res*. **2019**, *474*, 72-79.

(38) The calculated relative free energies between the classified conformer groups are inaccurate due to the overestimation of noncovalent interactions such as intramolecular hydrogen bonds. On the other hand, within each classified conformer group, the dihedral angles between vicinal hydrogens in the glucose moiety were very similar, and the position and number of intramolecular hydrogen bonds were the same. Therefore, it is believed that the weight-averaging of the calculated $J_{H,H}$ values according to the Boltzmann distribution based on the relative free energies within each classified conformer group provides reliable values.

(39) (a) Grimme, S.; Ehrlich, S.; Goerigk, L. Effect of the damping function in dispersion corrected density functional theory. *J. Comput. Chem*. **2011**, *32*, 1456-1465. (b) Grimme, S.; Antony, J.; Ehrlich, S.; Krieg, H. A consistent and accurate *ab initio* parametrization of density functional dispersion correction (DFT-D) for the 94 elements H-Pu. *J. Chem. Phys*. **2010**, *132*, 154104.

(40) Hayasaka, A.; Hashimoto, K.; Konno, K.; Tanaka, K.; Hashimoto, M. Isolation, Identification, and DFT-Based Conformational Analysis of sesquikarahanadienone and its congeners from freshwater Dothideomycetes *Neohelicascus aquaticus* KT4120. *Bull. Chem. Soc. Jpn*. **2022**, *95*, 833-845.

(41) Hashimoto *et al.* recently reported that functionals with the dispersion correction (e.g. ωB97X-D, B3LYP-D3)

overestimate intramolecular van der Waals interaction compared to classical functionals (e.g. B3LYP) for very flexible sesquiterpenes.[40]

(42) Since **6** was insoluble in D_2O, D_2O/DMSO-d_6 (9:1) was used as the NMR solvent.

(43) Nonaka, G.; Akazawa, M.; Nishioka, I. Two new ellagitannin metabolites, carpinusin and carpinusnin from *Carpinus laxiflora*. *Heterocycles* **1992**, *33*, 597-606.

(44) (a) Okuda, T.; Hatano, T.; Nitta, H.; Fujii, R. Hydrolysable tannins having enantiomeric dehydrohexahydroxydiphenoyl group: Revised structure of terchebin and structure of granatin B. *Tetrahedron Lett*. **1980**, *21*, 4361-4364. (b) Tanaka, T.; Nonaka, G.; Nishioka, I. Tannins and related compounds. C. Reaction of dehydrohexahydroxydiphenic acid esters with bases, and its application to the structure determination of pomegranate tannins, granatins A and B. *Chem. Pharm. Bull*. **1990**, *38*, 2424-2428. (c) Steinmetz, W. E. NMR assignment and characterization of proton exchange of the ellagitannin granatin B. *Magn. Reson. Chem*. **2010**, *48*, 565-570.

(45) Foo, L. Y. Amariin, a di-dehydrohexahydroxydiphenoyl hydrolysable tannin from *Phyllanthus amarus*. *Phytochemistry* **1993**, *33*, 487-491.

(46) Jaeschke, S. O.; Lindhorst, T. K.; Auer, A. Between two chairs: Combination of theory and experiment for the determination of the conformational dynamics of xylosides. *Chem.—Eur. J*. **2022**, *28*, e202201544.

(47) (a) Ma, J.-Y.; Zhou, X.; Fu, J.; Hu, T.; Or, P. M. Y.; Feng, R.; He, C.-Y.; Chen, W.-J.; Zhang, X.; Chen, Y.; Wang, Y.; Yeung, J. H. K. Metabolite profiling analysis of FR429, an ellagitannin purified from *Polygonum capitatum*, in rat and human liver microsomes, cytosol and rat primary hepatocytes *in vitro*. *Chem.-Biol. Interact*. **2014**, *220*, 33-40. (b) Yeggoni, D. P.; Rachamallu, A.; Subramanyam, R. A comparative binding mechanism between human serum albumin and α-1-acid glycoprotein with corilagin: biophysical and computational approach. *RSC Adv*. **2016**, *6*, 40225-40237. (c) Sobeh, M.; Mahmoud, M. F.; Hasan, R. A.; Abdelfattah, M. A. O.; Osman, S.; Rashid, H.; El-Shazly, A. M.; Wink, M. Chemical composition, antioxidant and hepatoprotective activities of methanol extracts from leaves of *Terminalia bellirica* and *Terminalia sericea* (Combretaceae). *PeerJ* **2019**, *7*, e6322. (d) Yang, Y.; Wang, X.; Gao, Y.; Niu, X. Insight into the dual inhibition mechanism of corilagin against MRSA serine/threonine phosphatase (Stp1) by molecular modeling. *ACS Omega* **2020**, *5*, 32959-32968. (e) Binette, V.; Côté, S.; Haddad, M.; Nguyen, P. T.; Bélanger, S.; Bourgault, S.; Ramassamy, C.; Gaudreault, R.; Mousseau, N. Corilagin and 1,3,6-tri-*O*-galloy-β-D-glucose: potential inhibitors of SARS-CoV-2 variants. *Phys. Chem. Chem. Phys*. **2021**, *23*, 14873-14888. (f) Yang, L. J.; Chen, R. H.; Hamdoun, S.; Coghi, P.; Ng, J. P. L.; Zhang, D. W.; Guo, X.; Xia, C.; Law, B. Y. K.; Wong, V. K. W. Corilagin prevents SARS-CoV-2 infection by targeting RBD-ACE2 binding. *Phytomedicine*, **2021**, *87*, 153591. (g) Li, Q.; Yi, D.; Lei, X.; Zhao, J.; Zhang, Y.; Cui, X.; Xiao, X.; Jiao, T.; Dong, X.; Zhao, X.; Zeng, H.; Liang, C.; Ren, L.; Guo, F.; Li, X.; Wang, J.; Cen, S. Corilagin inhibits SARS-CoV-2 replication by targeting viral RNA-dependent RNA polymerase. *Acta Pharm. Sin. B* **2021**, *11*, 1555-1567. (h) Sheng, Q.; Hou, X.; Wang, N.; Liu, M.; Zhu, H.; Deng, X.; Liang, X.; Chi, G. Corilagin: A novel antivirulence strategy to alleviate *Streptococcus pneumoniae* infection by diminishing pneumolysin oligomers. *Molecules* **2022**, *27*, 5063. (i) Pradeep, S.; Patil, S. M.; Dharmashekara, C.; Jain, A.; Ramu, R.; Shirahatti,P. S.; Mandal, S. P.; Reddy, P.; Srinivasa, C.; Patil, S. S.; Ortega-Castro, J.; Frau, J.; Flores-Holgúin, N.; Shivamallu, C.; Kollur, S. P.; Glossman-Mitnik, D. Molecular insights into the *in silico* discovery of corilagin from *Terminalia chebula* as a potential dual inhibitor of SARS-CoV-2 structural proteins. *J. Biomol. Struct. Dyn*. DOI: 10.1080/07391102.2022.2158943.

(48) (a) Feldman, K. S.; Sahasrabudhe, K.; Quideau, S.; Hunter, K. L.; Lawlor, M. D. Prospects and progress in ellagitannin synthesis. In *Plant Polyphenols 2: Chemistry, Biology, Pharmacology, Ecology*, Gross, G. G.; Hemingway, R. W.; Yoshida, T.; Branham, S. J., Eds.; Basic Life Sciences, Vol. 66; Springer, 1999; pp. 101-125. DOI: 10.1007/978-1-4615-4139-4_6. (b) Khanbabaee, K.; van Ree, T. Strategies for the synthesis of ellagitannins. *Synthesis* **2001**, 1585-1610; (c) Tanaka, T.; Kouno, I.; Nonaka, G. Biomimetic synthesis and related reactions of ellagitannins. In *Biomimetic Organic Synthesis*, Poupon, E.; Nay, B., Eds.; Vol. 2; Wiley-VCH, 2011; pp. 637-675. DOI: 10.1002/9783527634606.ch17. (d) Pouységu, L.; Deffieux, D.; Malik, G.; Natangelo, A.; Quideau, S. Synthesis of ellagitannin natural products. *Nat. Prod. Rep*. **2011**, *28*, 853-874. (e) Yamada, H.; Hirokane, T.; Asakura, N.; Kasai, Y.; Nagao, K. Strategies and methods for the total synthesis of ellagitannins. *Curr. Org. Chem*. **2012**, *16*, 578-604. (f) Yamada, H.; Hirokane, T.; Ikeuchi, K.; Wakamori, S. Fundamental methods in ellagitannin synthesis. *Nat. Prod. Commun*. **2017**, *12*, 1351-1358.

(49) (a) Yamada, H.; Nagao, K.; Dokei, K.; Kasai, Y.; Michihata, N. Total synthesis of (−)-corilagin. *J. Am. Chem. Soc*. **2008**, *130*, 7566-7567. (b) Yamashita, K.; Kume, Y.; Ashibe, S.; Puspita, C. A. D.; Tanigawa, K.; Michihata, N.; Wakamori, S.; Ikeuchi, K.; Yamada, H. Total synthesis of mallotusinin. *Chem.—Eur. J*. **2020**, *26*, 16408-16421.

Table of Contents artwork

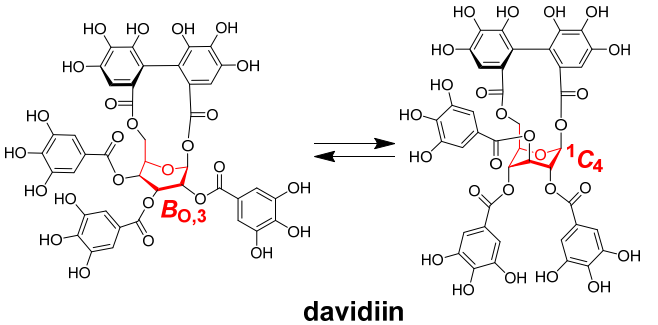

davidiin

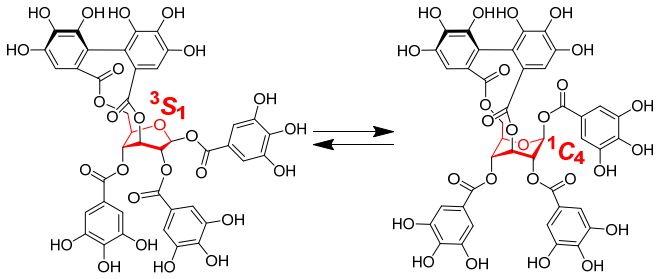

punicafolin